Ab initio study of the aromaticity of hydrogenated fullerenes

© G. Van Lier, F. De Proft, P. Geerlings

Vrije Universiteit Brussel, Department of General Chemistry,
B-1050 Brussel, Belgium

E-mail: pgeerlin@vub.ac.be

An analysis of the global and local aromaticity was made for a series of hydrogenated fullerenes of the type $C_{60}H_{2n}$ ($n = 1-6$) at *ab initio* HF(Hartree–Fock)/3-21G level of theory, the isomers considered being obtained with an octahedral addition pattern. The relation between this addition pattern and the magnetic properties was established, showing low aromatic regions to be preferred for addition. These results show that local aromaticity, as shown by nucleus-independent chemical shift, can be used to predict addition sites in these systems.

In many chemical reactions, fullerenes behave as electron deficient alkenes [1–3]. From its chemical properties, no global aromaticity is expected for C_{60}, and computed magnetic properties of closed-shell fullerenes show overall diamagnetic behaviour with sugnificant vatiations in local ring currents [4–10].

After computation studies of the chemical reactivity of hydrofullerenes and substituted hydrofullerenes of the type $C_{60}H_n$ [11], C_{60}HR [12] and C_{70}HR [13], the delocalisation that occured upon deprotonation of these systems has already been analysed [13,14]. With $C_{60}H_2$ and C_{60}Ht-Bu already being proven belonging to the most acidic hydrocarbons [15,16], further modelling of the chemical behaviour can be achieved upon modification of the functional group *R*, and serve as starting material for further synthesis [17].

Based on the expansion of C_{60} upon its three rotational axes, three distinct series of cylindrical fullerenes can be constructed. The C_5, C_3 and C_2 axes yield armchair, zigzag and chiral cylinders ("capped nanotubes") of signatures (5,5), (9,0) and (8,2), respectively [18]. These series have provided useful test sets for exploration of electronic structure [19–21] and elastic properties [22]. Also global and local aromaticities were recently described for these series [23]. Local aromaticity of a ring is described by its ability to support diamagnetic ring (i.e. diatropic) currents, which can be described by the nucleus-independent chemical shift (NICS) [24]. A more generally applicable model for local aromaticity, the so-called Pentagon–Proximity Model, could be derived, where the positioning of the pentagons in the system is seen to influence the whole pattern of local aromaticity for each system, as shown by *ab initio* NICS calculations. The overall magnetic structure can be understood in terms of a mechanical assembly of the counter-rotating rim and hub currents characteristics of circulene system such as coronene and corannulene [25].

In this work, we analyse the global and local aromaticity upon multiple octahedral addition of hydrogen to C_{60} in the series $C_{60}H_{2n}$ ($n = 1-6$). The relation between the local aromaticity, as denoted by NICS, with the addition pattern is highlighted.

After describing the computational details in Sect. 2, results will be detailed in Sect. 3 for the global (Sect. 3.1.) and the local aromaticities (Sect. 3.2.), and the relation with the addition pattern is discussed (Sect. 3.3.). Conclusions will be drawn in Sect. 4, together with the perspectives for further investigations.

1. Computational details

Structures were fully optimized at the AM1 (Austin Model 1) semiempirical level [26] using the MNDO (Modified Neglect of Differential Overlap) program [27] as a part of the graphical user interface UNICHEM [28].

Global aromaticities were analyzed by considering HOMO-LUMO gaps and molecular magnetisablities. To investigate local aromaticities, NICS were calculated at all geometrical ring centers [24].

All property calculations were performed at the *ab initio* HF/3-21G level using GAUSSIAN98 [29]. NICS values for all rings were computed at symmetry-distinct ring centers, using the GIAO (Gauge-Independent Atomic Orbital) method (for a review on the different methods to analyse magnetic properties we refer to [30] and the references therein), and magnetisabilities were evaluated at the same level using the CSGT (Continious Set of Gange Transformation) methodology [30].

2. Results and Discussion

2.1. Global Aromaticity. All the systems studied in this work are a part of the $C_{60}H_{2n}$ ($n = 1-6$) series, considering octahedral addition patterns. They are listed in Table 1, together with their symmetries and numbering [31]. All systems are constructed from addition to one or more of six octahedrally positioned hexagon-hexagon edges, each part of a distinct pyracylenic unit. Also the calculated energies are given in Table 1, with isomers listed in order of increasing energy, found to be consistent with previous semi-empirical calculations [32]. As different isomers can be formed from the previous series member, following relations exist between isomers: starting from 1,2-$C_{60}H_2$, two distinct isomers for $C_{60}H_4$ (systems (3) and (4)) can be formed.

Further addition to the former can yield all three $C_{60}H_6$ isomers, but the latter can only give (6) and (7). Finally, the first $C_{60}H_6$ isomer (5) can only form (8), whereas the others

Table 1. Symmetries and numbering [31] for all studied systems, together with their energies (in a. u.), calculated at *ab initio* 3-21G level

System	Symmetry	Numbering	Energy
C_{60} (1)	I_h		−2259.0405
$C_{60}H_2$ (2)	C_{2v}	1, 2	−2260.2050
$C_{60}H_4$ (3)	C_s	1, 2; 22, 23	−2261.3770
$C_{60}H_4$ (4)	D_{2h}	1, 2; 55, 60	−2261.3758
$C_{60}H_6$ (5)	C_3	1, 2; 16, 36; 22, 23	−2262.5491
$C_{60}H_6$ (6)	C_{2v}	1, 2; 22, 23; 31, 32	−2262.5474
$C_{60}H_6$ (7)	C_{2v}	1, 2; 22, 23; 55, 60	−2262.5466
$C_{60}H_8$ (8)	C_s	1, 2; 18, 36; 22, 23; 27, 45	−2263.7187
$C_{60}H_8$ (9)	D_{2h}	1, 2; 22, 23; 31, 32; 55, 60	−2263.7157
$C_{60}H_{10}$ (10)	C_{2v}	1, 2; 18, 36; 22, 23; 27, 45; 55, 60	−2264.8872
$C_{60}H_{12}$ (11)	T_h	1, 2; 18, 36; 22, 23; 27, 45; 31, 32; 55, 60	−2266.0552

Table 2. HOMO and LUMO energies, band gap Δ (a. u.), the number of conjugated atoms and the *T*-value in a. u., and the magnetisabilities in ppm, calculated at *ab initio* 3-21G level

Sysmem	ε_{HOMO}	ε_{LUMO}	Δ	# conjugated atoms	*T*-value	Magnetisability
C_{60} (1)	−0.3061	−0.0247	0.2814	60	16.9	−342
$C_{60}H_2$ (2)	−0.2863	−0.0240	0.2623	58	15.2	−360
$C_{60}H_4$ (3)	−0.2786	−0.0138	0.2648	56	14.8	−381
$C_{60}H_4$ (4)	−0.2761	−0.0206	0.2555	56	14.3	−362
$C_{60}H_6$ (5)	−0.2879	−0.0076	0.2803	54	15.1	−401
$C_{60}H_6$ (6)	−0.2680	−0.0020	0.2660	54	14.4	−380
$C_{60}H_6$ (7)	−0.2710	−0.0104	0.2606	54	14.1	−376
$C_{60}H_8$ (8)	−0.2808	−0.0137	0.2671	52	13.9	−396
$C_{60}H_8$ (9)	−0.2600	+0.0010	0.2609	52	13.6	−369
$C_{60}H_{10}$ (10)	−0.2760	−0.0242	0.2518	50	12.6	−385
$C_{60}H_{12}$ (11)	−0.2728	0.0424	0.2304	48	11.1	−369

can each form both $C_{60}H_8$ isomers, which in turn yield the unique isomers for $C_{60}H_{10}$ and $C_{60}H_{12}$ upon further hydrogenation.

The global aromaticity for these system was described with the HOMO-LUMO gap, the kinetic stability *T* [33], and molecular magnetisabilities, as given in Table 2. As the HOMO-LUMO gap, Δ, is an estimate of the chemical hardness [34], and the latter property has been proposed as a measure of the global aromaticity [34–38] (for recent reviews on the use of DFT (Density Function Theory) — based reactivity and stability descriptors, see references [39–41], we can see from Table 2 that the trend in energy (Table 1) coincides with the band gap. Indeep, the lower the energy, the higher the band gap, indicating a higher global aromaticity. From these most stable isomers, we can see a clear increase in band gap up to $C_{60}H_6$ (system (5)), followed by a decrease upon increasing hydrogenation. The magnetisabilities show exactly the same trend, and also show decreasing global aromaticity with increasing energy when comparing isomers.

The size dependence of the band gap can be removed by simple multiplication of Δ by the number of conjugated atoms to give the so-called "kinetic stability", *T* [33]. This quantity was recently found to correlate with the minimum Bond Resonance Energy (min BRE) in a fullerene, and both *T* and min BRE have been proposed as useful measures for the chemical reactivity of fullerene systems [33]. The kinetic stability (given in Table 2, together with the number of conjugated atoms) gives a general decrease between and within isomers, but with (5) again as a more aromatic exception.

In the next Section, local aromaticity will be analysed in order to gain insight in the possible addition patterns.

2.2. Local Aromaticity. In Figure modified Schlegel forms are presented with the NICS, calculated for all rings at the geometrical ring centers, as an evaluation of the local aromaticity. From these values, significant differences with the values for C_{60} can be seen in the addition region (the NICS of C_{60} are +5.1 ppm for the pentagons and −6.8 ppm for the hexagons). Starting from a picture of diamagnetic hexagons and paramagnetic pentagons, addition of two hydrogens on a bond to form 1,2-$C_{60}H_2$, makes the four rings of the pyracylenic unit to become non-aromatic. On the other hand, 4 benzenoid rings are created, adjacent to this pyracylenic unit. Adding another pair of hydrogens can now be expected to occur in such a way as to reinforce this local magnetic pattern, rather than to undo it. As seen from the NICS for $C_{60}H_4$, again 4 benzenoid rings are now created around the second added pair. Two of these are shared with the first addition in (3), indeed showing higher

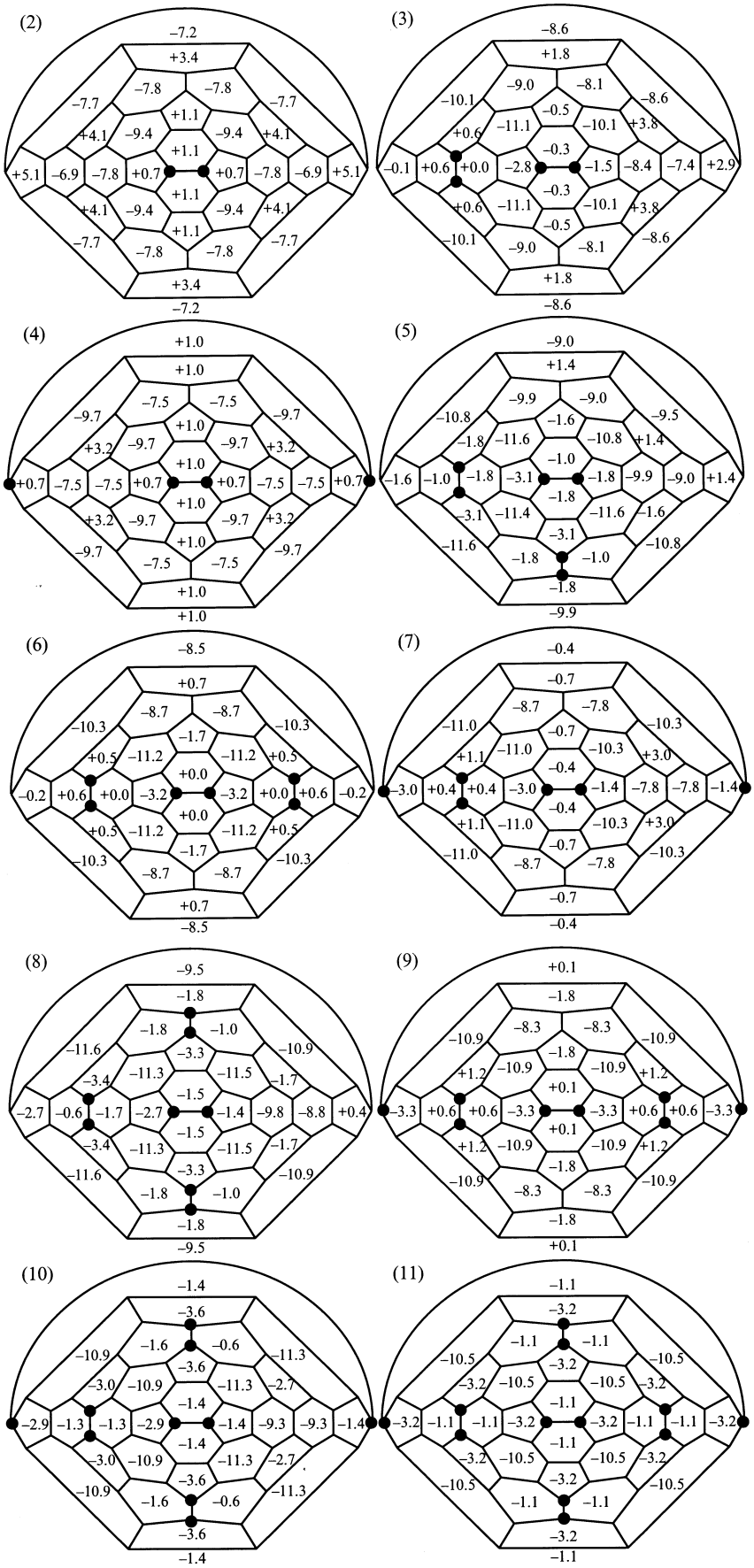

NICS values obtained for the various fullerenes in the 3-21G basis at the AMI geometries (ppm) (numbering, see Table 1).

NICS, as compared to (4). The same applies to the possible isomers of $C_{60}H_6$ and $C_{60}H_8$, showing more negative NICS, and thus higher local aromaticity, for the isomers with higher global aromaticity (see Sect. 3.1). Furthermore, we can see three benzonid rings having the highest NICS value found (-11.6 ppm) for isomer (5) of $C_{60}H_6$, consistent with the results found for the global aromaticity (see Table 1).

Upon increasing octahedral addition, a pattern appears where 8 isolated benzenoid rings are created, surrounded by non-aromatic pentagons and hexagons at the hydrogenated pyracylenic units. Such substructures were already detected in the analysis of the local aromaticity for cylindrical fullerenes [23], described in terms of recent results for coronene and corannulene [25].

2.3. Relation with the addition pattern. From a chemical point of view, addition to the C_{60} cage will occur at the most reactive bond, expected to be situated in the electronically most localised region of the system. Formulated in terms of magnetic properties, such a region could be expected to show the lowest local aromaticity or antiaromaticity, marked by higher NICS values for the hexagons and lower NICS values for the pentagons involved in the corresponding addition site. From the results in Figure, it is seen that consecutive octahedral addition indeed occuring at the pyracylenic site with the pentagon with lowest NICS, will yield the isomer having the highest global aromaticity. Furthermore, in most cases, this addition site also involves the hexagon with lowest aromaticity (less negative NICS). In this way, the site having the lowest local delocalisation is indeed found to yield, upon addition, the most stable isomer, being the addition product with highest global aromaticity.

The global and local aromaticities were described for a number of hydrogenated fullerenes of the type $C_{60}H_{2n}$ ($n = 1-6$), obtained by octahedral addition. First increasing in global aromatic character upon increasing hydrogenation, a decrease is noted from $C_{60}H_6$ on, considering the most stable isomer of each series member, having the highest global aromaticity as well as the lowest energy. From the results for the local aromaticity, as predicted by NICS, calculated at all geometrical ring centers, significant variations can be seen for the hydrogenated fullerenes as compared to C_{60}. Upon higher hydrogenation, a set of benzenoid rings can be detected, with higher local aromaticities occurring for the isomers with higher global aromaticity. Furthermore, the additions are seen to occur at the site with lowest local delocalisation, as described by NICS. Indeed, consecutive octahedral additions occurring at the site comprising the less anti-aromatic pentagon, gives the most stable isomer of the next series member.

From these results it can be stated that consideration of the local aromaticity, as monitored by NICS, can contribute to predict multiple addition sites for substituted closed-shell fullerenes. As NICS describes the local aromaticity of the system, regions with smaller aromaticity, and thus smaller delocalisation are mapped. Together with considerations of the aromaticity pattern of the addition product, a clear evaluation of the preferential isomer can be made. In further investigations, this methodology will be applied to a broad range of functionalised fullerenes, including C_{70} and C_{76} derivatives, as well as charged fullerenes.

The authors would like to thank Prof. P.W. Fowler (University of Exeter, UK) for many enlightening discussions.

References

[1] A. Hirsch. The Chemistry of the Fullerenes. Georg Thieme Verlag, Stuttgart (1994).
[2] R. Taylor. The Chemistry of Fullerenes. World Scientific Pub Co (1996).
[3] R. Taylor. Lecture Notes on Fullerene Chemistry. A Handbook for Chemists. Imperial College Press (1999).
[4] P.W. Fowler, P. Lazzeretti, R. Zanasi. Chem. Phys. Lett. **165**, 79 (1990).
[5] P.W. Fowler, P. Lazzaretti, M. Malagoli, R. Zanasi. Chem. Phys. Lett. **179**, 174 (1991).
[6] R.C. Haddon. Science **261**, 1545 (1993).
[7] R.C. Haddon, L.F. Schneemeyer, J.V. Waszczak, S.H. Glarum, R. Tycko, G. Dabbagh, A.R. Kortan, A.J. Muller, A.M. Mujsce, M.J. Rosseinsky, S.M. Zahurak, A.V. Makhija, F.A. Thiel, K. Raghavachari, E. Cockayne, V. Elser. Nature **350**, 46 (1993).
[8] R.C. Haddon, A. Pasquarello. Phys. Rev. **B50**, 16 459 (1994).
[9] M. Bühl. Chem. Eur. J. **4**, 734 (1998).
[10] M. Bühl, A. Hirsch. Chem. Rev. **101**, 1 153 (2001).
[11] K. Choho, G. Van Lier, G. Van De Woude, P. Geerlings. J. Chem. Soc. Perkin Trans. **2**, 1723 (1996).
[12] G. Van Lier, B. Safi, P. Geerlings. Phys. Chem. Solids **58**, 1719 (1997).
[13] G. Van Lier, P. Geerlings. Chem. Phys. Lett. **289**, 591 (1998).
[14] G. Van Lier, B. Safi, P. Geerlings. J. Chem. Soc. Perkin Trans. **2**, 349 (1998).
[15] P.J. Fagan, P.J. Krisic, D.H. Evans, S.A. Lerke, E. Johnston. J. Am. Chem. Soc. **114**, 9697 (1992).
[16] M.E. Nyazymbetov, D.H. Evans, S.A. Lerke, P.A. Cahill, C.C. Henderson. J. Phys. Chem. **98**, 13 093 (1994).
[17] T. Kitagawa, K. Takeuchi. Bull. Chem. Soc. Jpn. **74**, 785 (2001).
[18] M.S. Dresselhaus, G. Dresselhaus, P.C. Eklund. Science of Fullerenes and Carbon Nanotubes. Academic Press, Inc.: San Diego, California, USA (1995).
[19] P.W. Fowler. J. Chem. Soc. Faraday Trans. **86**, 2073 (1990).
[20] P.W. Fowler. J. Phys. Chem. Solids **12**, 1825 (1993).
[21] P.W. Fowler, D.E. Manolopoulos. An Atlas of Fullerenes. Oxford University Press, Oxford (1995). Vol. 30.
[22] G. Van Lier, C. Van Alsenoy, V. Van Doren, P. Geerlings. Chem. Phys. Lett. **326**, 181 (2000).
[23] G. Van Lier, P.W. Fowler, F. De Proft, P. Geerlings. J. Phys. Chem., submitted.
[24] P.v.R. Schleyer, C. Maerker, A. Dransfeld, H. Jiao, N.J.R. van Eikema Hommes. J. Am. Chem. Soc. **118**, 6317 (1996).
[25] E. Steiner, P.W. Fowler, L.W. Lenneskens. Angew. Chem. Int. Ed. **40**, 362 (2001).
[26] J.P.P. Stewart. J. Comp. Aid. Mol. Des. **4**, 1 (1990).
[27] M.J.S. Dewar, W. Thiel. J. Am. Chem. Soc. **99**, 4899 (1977).
[28] C.R.I. UniChem. Eagon MN (1994).

[29] M.J. Frisch, G.W. Trucks, H.B. Schlegel, G.E. Scuseria, M.A. Robb, J.R. Cheeseman, V.G. Zakrzewski, J.A. Montgomery, Jr., R.E. Stratmann, J.C. Burant, S. Dapprich, J.M. Millam, A.D. Daniels, K.N. Kudin, M.C. Strain, O. Farkas, J. Tomasi, V. Barone, M. Cossi, R. Cammi, B. Mennucci, C. Pomelli, C. Adamo, S. Clifford, J. Ochterski, G.A. Petersson, P.Y. Ayala, Q. Cui, K. Morokuma, D.K. Malick, A.D. Rabuck, K. Raghavachari, J.B. Foresman, J. Cioslowski, J.V. Ortiz, A.G. Baboul, B.B. Stefanov, G. Liu, A. Liashenko, P. Piskorz, I. Komaromi, R. Gomperts, R.L. Martin, D.J. Fox, T. Keith, M.A. Al-Laham, C.Y. Peng, A. Nanyakkara, M. Challacombe, P.M.W. Gill, B. Johnson, W. Chen, M.W. Wong, J.L. Andres, C. Gonzalez, M. Head-Gordon, E.S. Replogle, J.A. Pople. Gaussian 98, Revision A. 9. Gaussian Inc., Pittsburgh PA (1998).
[30] T. Helgaker, M. Jaszunski, K. Ruud. Chem. Rev. **99**, 293 (1999).
[31] R. Taylor. J. Chem. Soc. Perkin Trans. **2**, 813 (1993).
[32] B.W. Clare, D.L. Kepert. J. Mol. Struct. (Theochem). **281**, 45 (1993).
[33] J. Aihara. Phys. Chem. Chem. Phys. **2**, 3121 (2000).
[34] F. De Proft, P. Geerlings. Chem. Rev. **101**, 1451 (2001).
[35] Z.X. Zhou, R.G. Parr, J.F. Garst. Tetrahedron Lett. **29**, 4843 (1988).
[36] Z.X. Zhou, R.G. Parr. J. Am. Chem. Soc. **111**, 7371 (1989).
[37] Z.X. Zhou, R.G. Parr. J. Am. Chem. Soc. **112**, 5720 (1990).
[38] R. Balawender, L. Komorowski, F. De Proft, P. Geerlings. J. Phys. Chem. **A102**, 9912 (1998).
[39] H. Chermette. J. Comput. Chem. **20**, 129 (1990).
[40] P. Geerlings, F. De Proft, W. Langenaeker. Adv. Quant. Chem. **33**, 303 (1999).
[41] P. Geerlings, F. De Proft. Int. J. Quantum Chem. **80**, 227 (2000).